Acetylcholinesterase Inhibitors: Synthesis and Structure−Activity Relationships of ω-[*N*-Methyl-*N*-(3-alkylcarbamoyloxyphenyl)-methyl]aminoalkoxyheteroaryl Derivatives

Angela Rampa,[†] Alessandra Bisi,[†] Piero Valenti,*[,†] Maurizio Recanatini,[†] Andrea Cavalli,[†] Vincenza Andrisano,[†] Vanni Cavrini,[†] Lorena Fin,[‡] Alessandro Buriani,[‡,§] and Pietro Giusti[‡]

Department of Pharmaceutical Sciences, University of Bologna, Via Belmeloro 6, 40126 Bologna, Italy, Department of Pharmacology, University of Padova, Largo Meneghetti 2, 35131 Padova, Italy, and Cooperative Research & Innovation, Via Leopardi 14, Sovizzo, VI, Italy

Received February 17, 1998

Acetylcholinesterase (AChE) inhibitors are one of the most actively investigated classes of compounds in the search for an effective treatment of Alzheimer's disease. This work describes the synthesis, AChE inhibitory activity, and structure−activity relationships of some compounds related to a recently discovered series of AChE inhibitors: the ω-[*N*-methyl-*N*-(3-alkylcarbamoyloxyphenyl)methyl]aminoalkoxyxanthen-9-ones. The influence of structural variations on the inhibitory potency was carefully investigated by modifying different parts of the parent molecule, and a theoretical model of the binding of one representative compound to the enzyme was developed. The biological properties of the series were investigated in some detail by considering not only the activity on isolated enzyme but the selectivity with respect to butyrylcholinesterase (BuChE) and the in vitro inhibitory activity on rat cerebral cortex as well. Some of the newly synthesized derivatives, when tested on isolated and/or AChE-enriched rat brain cortex fraction, displayed a selective inhibitory activity and were more active than physostigmine. In particular, compound **13**, an azaxanthone derivative, displayed the best rat cortex AChE inhibition (190-fold higher than physostigmine), as well as a high degree of enzyme selectivity (over 60-fold more selective for AChE than for BuChE). When tested in the isolated enzyme, compound **13** was less active, suggesting some differences either in drug availability/biotransformation or in the inhibitor-sensitive residues of the enzyme when biologically positioned in rat brain membranes.

Senile dementia of the Alzheimer type (SDAT) is a neurodegenerative disease associated with neuronal damage involving several neurotransmitter systems of the brain. One of the most pronounced functional deficits involves cholinergic neurons of the central nervous system (CNS). For years cholinergic enhancement has been considered a sensible therapeutic approach for improving brain functions in SDAT patients. CNS cholinergic enhancement can be achieved with the use of acetylcholine (ACh) precursors, muscarinic agonists, or acetylcholinesterase (AChE) inhibitors.[1]

Unfortunately, efforts to develop drugs possessing this last activity have been so far hampered by the short persistency and/or low specificity of the pharmacological effect.[2] Many anticholinesterase agents, in fact, also inhibit butyrylcholinesterase (BuChE) which is found in both plasma and brain. This inhibition can lead to adverse peripheral side effects.[2] Further research is thus needed to design new molecules with improved activity, and much attention has been focused on AChE inhibitors such as 1,2,3,4-tetrahydro-9-aminoacridine (tacrine),[2,3] physostigmine and its analogues,[4] and *N*-benzylpiperidines.[5]

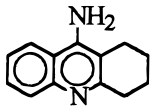

Tacrine

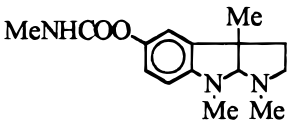

Physostigmine

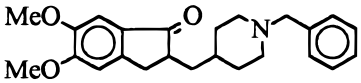

E2020

It has long been postulated that the active site of AChE contains an anionic as well as an esteratic site and a hydrophobic binding site (HBS-l). However, from the X-ray analysis of AChE from *Torpedo californica* reported by Sussman et al.,[6] it was shown that the quaternary nitrogen of ACh binds strongly with the π electrons of the Trp84 group. According to this model, Chen et al.[7] hypothesized that the carbonyl center of physostigmine and other carbamates interacts with the enzyme via the Ser-His-Glu catalytic triad and the quaternary nitrogen interacts with neighboring aromatic residues. One of these residues might correspond to the second hydrophobic binding site (HBS-2) proposed by Ishihara et al.[8] On this basis, in a previous paper,[9]

[†] University of Bologna.
[‡] University of Padova.
[§] Cooperative Research & Innovation.

S0022-2623(98)01004-8 CCC: $15.00
Published on Web 09/12/1998

Scheme 1[a]

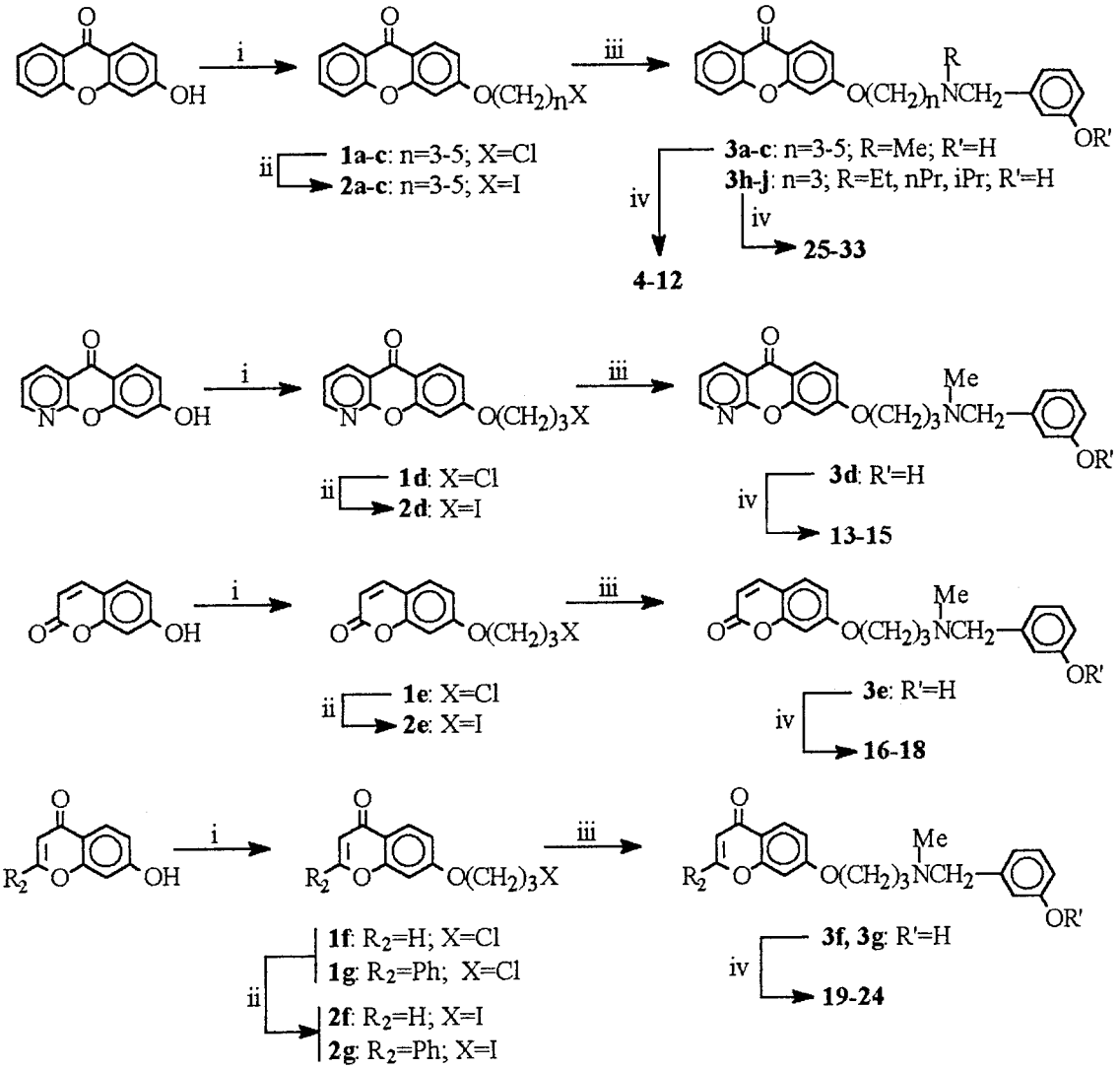

[a] Reagents: (i) $Br(CH_2)_nCl$, K_2CO_3 reflux, 24 h; (ii) NaI, methyl ethyl ketone, reflux 4 h; (iii) *N*-(3-hydroxybenzyl)alkylamine, reflux, 15 h; (iv) alkyl isocyanate, NaH, room temperature, 24 h.

we designed some xanthone analogues of general formula

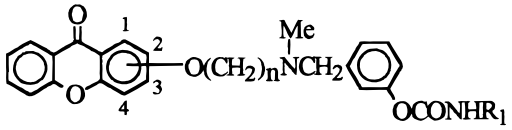

where the alkoxy chain occupies, alternatively, the 2, 3, and 4 positions of the xanthone moiety and has a variable length. The compounds were then evaluated for anti-AChE activity, and some were indeed more active than physostigmine, taken as reference molecule. Optimum activity was associated with the 3 side chain position on the xanthone nucleus and with a three-carbon chain length separating the xanthenonyloxy moiety from the nitrogen atom of the benzylaminic moiety. Encouraged by such results, we synthesized several related compounds with the aim of identifying key structural elements involved in the interactions with AChE, which could endow the new molecules with a better pharmacological activity.

The anti-AChE activity of all the new compounds was first tested using the isolated enzyme. An attempt to rationalize the structure−activity relationships of the series was carried out, and a theoretical model of the binding mode of the most active compound was developed. Some of the compounds displaying an activity superior or equal to physostigmine were also examined for enzymatic selectivity, by comparing their inhibitory activity on isolated AChE with that exerted on isolated BuChE. The AChE inhibitory activity of the most interesting compounds was further analyzed on rat brain cortex fractions enriched with AChE activity.

Chemistry

The synthesis of the compounds was accomplished as illustrated in Scheme 1. The selected hydroxy derivatives were treated with 1-bromo-ω-chloroalkanes in the presence of K_2CO_3 to afford ω-chloroalkoxy derivatives **1a**−**g**, which were treated with NaI in refluxing methyl ethyl ketone to give the corresponding ω-iodoalkoxy derivatives **2a**−**g.** Compounds **2a**−**g** were condensed with the selected *N*-(3-hydroxy)benzylalkylamine to afford compounds **3a**−**j** and then treated with the selected alkyl isocyanate to give the studied compounds **4**−**33**.

Table 1. Physicochemical and Analytical Data of the Compounds Studied

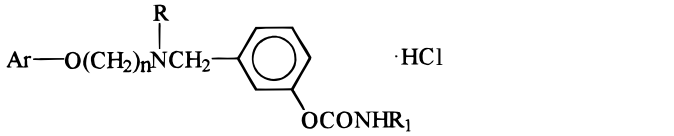

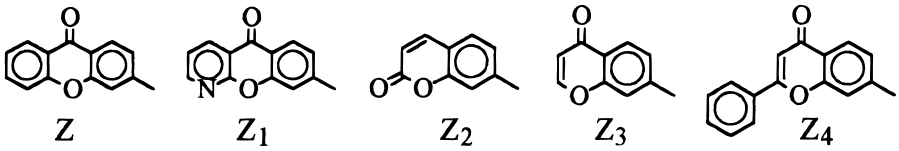

compd	Ar	*n*	R	R_1	mp (°C)[a]	yield (%)	formula	analysis
4	Z	4	Me	Me	108−110	45	$C_{27}H_{29}ClN_2O_5$	C, H, N
5	Z	4	Me	*n*-Hep	93−95	40	$C_{33}H_{41}ClN_2O_5$	C, H, N
6	Z	5	Me	Me	110−112	50	$C_{28}H_{29}N_2O_5$[b]	C, H, N
7	Z	5	Me	*n*-Hep	135−137	30	$C_{34}H_{43}ClN_2O_5$	C, H, N
8	Z	3	Me	Me	101−103	55	$C_{26}H_{26}N_2O_5$[b]	C, H, N
9	Z	3	Me	Et	118−120	40	$C_{27}H_{28}N_2O_5$[b]	C, H, N
10	Z	3	Me	*n*-Pr	91−93	60	$C_{28}H_{30}N_2O_5$[b]	C, H, N
11	Z	3	Me	*n*-Bu	67−68	35	$C_{29}H_{32}N_2O_5$[b]	C, H, N
12	Z	3	Me	Ph	128−130	70	$C_{31}H_{29}ClN_2O_5$	C, H, N
13	Z_1	3	Me	Me	213−215	80	$C_{25}H_{26}ClN_3O_5$	C, H, N
14	Z_1	3	Me	*n*-Bu	174−176	70	$C_{28}H_{32}ClN_3O_5$	C, H, N
15	Z_1	3	Me	*n*-Hep	185−187	50	$C_{31}H_{38}ClN_3O_5$	C, H, N
16	Z_2	3	Me	Me	166−168	90	$C_{22}H_{25}ClN_2O_5$	C, H, N
17	Z_2	3	Me	*n*-Bu	183−184	50	$C_{25}H_{31}ClN_2O_5$	C, H, N
18	Z_2	3	Me	*n*-Hep	184−186	70	$C_{28}H_{37}ClN_2O_5$	C, H, N
19	Z_3	3	Me	Me	128−130	30	$C_{22}H_{25}ClN_2O_5$	C, H, N
20	Z_3	3	Me	*n*-Pr	90−92	40	$C_{24}H_{29}ClN_2O_5$	C, H, N
21	Z_3	3	Me	*n*-Hep	111−113	60	$C_{28}H_{37}ClN_2O_5$	C, H, N
22	Z_4	3	Me	Me	ND[c]	70	$C_{28}H_{29}ClN_2O_5$	C, H, N
23	Z_4	3	Me	*n*-Bu	110−111	80	$C_{31}H_{35}ClN_2O_5$	C, H, N
24	Z_4	3	Me	*n*-Hep	155−157	70	$C_{34}H_{41}ClN_2O_5$	C, H, N
25	Z	3	Et	Me	103−105	60	$C_{27}H_{28}N_2O_5$[b]	C, H, N
26	Z	3	Et	*n*-Bu	60−62	65	$C_{30}H_{34}N_2O_5$[b]	C, H, N
27	Z	3	Et	*n*-Hep	170−172	50	$C_{33}H_{41}ClN_2O_5$	C, H, N
28	Z	3	*n*-Pr	Me	125−127	70	$C_{28}H_{31}ClN_2O_5$	C, H, N
29	Z	3	*n*-Pr	*n*-Bu	114−116	55	$C_{31}H_{37}ClN_2O_5$	C, H, N
30	Z	3	*n*-Pr	*n*-Hep	172−174	40	$C_{34}H_{43}ClN_2O_5$	C, H, N
31	Z	3	*i*-Pr	Me	84−86	70	$C_{28}H_{30}N_2O_5$[b]	C, H, N
32	Z	3	*i*-Pr	*n*-Bu	85−87	65	$C_{31}H_{36}N_2O_5$[b]	C, H, N
33	Z	3	*i*-Pr	*n*-Hep	155−157	40	$C_{34}H_{43}ClN_2O_5$	C, H, N

[a] Crystallizing solvent: methanol−ether. [b] Free base (crystallizing from ligroin). [c] Hygroscopic solid.

The *N*-(3-hydroxy)benzylalkylamines were prepared by condensation of 3-hydroxybenzaldehyde and the selected amine followed by $NaBH_4$ reduction.

The structure and the physicochemical and analytical data of compounds **4**−**33** are reported in Table 1.

Results

Structure−Activity Relationships of the AChE Inhibition. Values for the inhibitory activity of the compounds against isolated AChE were expressed as $IC_{50} \pm SD$ and are reported in Table 2. In view of a clearer presentation of the structure−activity relationships (SAR) of the series, four structural features were identified in the general structure of the compounds studied: (a) the linker between the heteroaryloxy moiety and the basic nitrogen (*n*); (b) the N-substituent on the carbamoyl group (R_1); (c) the heteroaryloxy moiety (Ar), and (d) the N-substituent on the basic nitrogen (R).

(a) The Linker (*n*). Compounds **4**−**7** show a variable chain (four or five carbon units) separating the heteroaryloxy moiety from the nitrogen atom of benzylaminic moiety. These compounds were prepared in order to find the optimal length of this chain. Indeed, the best inhibitory activity on isolated AChE is associated with a three-carbon chain length ($n = 3$, compound **8**, $IC_{50} = 0.30 \pm 0.01$ nM), and increasing the chain length to four carbons ($n = 4$) results in a large reduction of activity (compound **4**). Interestingly, a chain length of five carbons ($n = 5$) leads to a recovery of the inhibitory activity (compound **6**). The association of the best activity with $n = 3$ is in agreement with what we had seen previously,[9] and for the following SAR studies we proceeded maintaining $n = 3$.

(b) The Carbamoyl Substituent (R_1). Various substituents on the carbamoyl moiety were examined in order to study their influence on the activity. It is known that the length of alkyl groups in that position should influence the rate constant of AChE inhibition,[10] and this aspect will be considered in a subsequent section. Replacing the methyl group of **4** and **6** with a *n*-heptyl group (compounds **5** and **7**, respectively) strongly decreases the inhibitory activity. When R_1 is an alkyl group and $n = 3$, optimum activity is associated with a methyl (compound **8** is 45-fold more active than physostigmine) and the anti-AChE activity decreases when it is changed into an ethyl, *n*-propyl, or *n*-butyl (compounds **9**−**11**). A phenyl group in the carbamoyl moiety gives a molecule (compound **12**) which, though still less

Table 2. Inhibitory Activity on Isolated AChE and BuChE, Ratio of IC_{50}, and Inhibitory Activity on Rat Brain AChE of the Compounds Studied

compd	Ar[a]	*n*	R	R_1	IC_{50} (nM) AChE	IC_{50} (nM) BuChE	ratio IC_{50} (BuChE/AChE)	IC_{50} (nM) rat brain AChE
4	Z	4	Me	Me	37 ± 5			
5	Z	4	Me	*n*-Hep	100 ± 10			
6	Z	5	Me	Me	0.82 ± 0.07	83 ± 3	101	>100
7	Z	5	Me	*n*-Hep	100 ± 20			
8	Z	3	Me	Me	0.30 ± 0.01	48 ± 4	160	20 ± 20
9	Z	3	Me	Et	13 ± 1	26 ± 3	2	40 ± 20
10	Z	3	Me	*n*-Pr	28 ± 4			
11	Z	3	Me	*n*-Bu	36 ± 2			
12	Z	3	Me	Ph	2.8 ± 0.2	200 ± 10	71.4	>1000
13	Z_1	3	Me	Me	1.1 ± 0.2	76 ± 6	69.1	0.009 ± 0.005
14	Z_1	3	Me	*n*-Bu	8.9 ± 0.4	24 ± 2	2.7	70 ± 30
15	Z_1	3	Me	*n*-Hep	42 ± 2			
16	Z_2	3	Me	Me	5.7 ± 0.5	3.6 ± 0.2	0.6	1.5 ± 0.7
17	Z_2	3	Me	*n*-Bu	14 ± 1			
18	Z_2	3	Me	*n*-Hep	13 ± 0.2	65 ± 3	5	2 ± 2
19	Z_3	3	Me	Me	8.9 ± 0.2			
20	Z_3	3	Me	*n*-Pr	250 ± 10			
21	Z_3	3	Me	*n*-Hep	21 ± 1			
22	Z_4	3	Me	Me	5.7 ± 0.7	47 ± 4	8.2	0.6 ± 0.5
23	Z_4	3	Me	*n*-Bu	31 ± 2			
24	Z_4	3	Me	*n*-Hep	68 ± 3			
25	Z	3	Et	Me	0.56 ± 0.05	21 ± 2	37.5	4 ± 3
26	Z	3	Et	*n*-Bu	8.6 ± 0.05			
27	Z	3	Et	*n*-Hep	160 ± 30			
28	Z	3	*n*-Pr	Me	4.0 ± 1			
29	Z	3	*n*-Pr	*n*-Bu	70 ± 20			
30	Z	3	*n*-Pr	*n*-Hep	400 ± 60			
31	Z	3	*i*-Pr	Me	0.7 ± 0.1			
32	Z	3	*i*-Pr	*n*-Bu	100 ± 10			
33	Z	3	*i*-Pr	*n*-Hep	170 ± 30			
phys.					14 ± 0.2	23 ± 1	1.6	2 ± 1

[a] See top of Table 1.

active than that with the methyl group, is more active than those with longer alkyl chains. When the heteroaryl nucleus is different from the xanthone (compounds **13**−**24**), increasing the length of the carbamic alkyl substituent generally leads to a decrease of activity that not always depends on the number of carbon units. In the coumarin subset (compounds **16**−**18**), the *n*-butyl and *n*-heptyl derivatives are equally potent, while the chromone derivatives (compounds **19**−**21**) show variable activity, i.e., the *n*-propyl derivative is less active than the *n*-heptyl one.

(c) The Heteroaryloxy Moiety (Ar). In the subset of compounds **13**−**24**, the xanthone nucleus was replaced by the bioisoster azaxanthone (compounds **13**−**15**) or by coumarin (compounds **16**−**18**), chromone (compounds **19**−**21**), and flavone (compounds **22**−**24**) moieties. The rationale for these modifications is based on the hypothesis that the xanthone moiety can be successfully replaced with structurally related oxygen heterocycles such as coumarin, chromone, and flavone. In fact, in a number of cases this replacement allowed us to obtain important results with regard to analeptics,[11] adrenergic-β-blocking agents,[12] clofibrate-like hypolipemic drugs,[13] and more recently, bradycardic[14] and antitumor drugs.[15−17] Some of the compounds of the subset are more active than physostigmine in inhibiting isolated AChE activity, and in all the cases, the best activity is associated with a methyl group in the carbamoyl fragment (compounds **13**, **16**, **19**, and **22**). Compound **13** is the best of this series, and it is 13-fold more active than physostigmine but 4-fold less active than the xanthone analogue **8**.

(d) The Amine Substituent (R). Finally, the substituent on the protonable amine group was studied by replacing the methyl group of the basic nitrogen with ethyl, *n*-propyl, and *i*-propyl groups (compounds **25**−**33**). It is evident that these modifications, which increase both lipophilicity and steric hindrance of the molecules, are not favorable and, in some cases, even detrimental for the inhibitory activity on isolated AChE. Only compounds **25** and **31** show IC_{50} values comparable with **8** (IC_{50} = 0.30 ± 0.01 nM). In a recent paper,[18] the hypothesis was formulated that lipophilicity that is too high might prevent the AChE inhibitors from reaching their binding site, due to possible interactions with the hydrophobic walls of the active site gorge. On the other hand, steric effects might play a role in determining the differences in activity, at least for compounds with the same R_1. For instance, when R_1 is methyl or *n*-heptyl (compounds **25**, **27**, **28**, **30**, **31**, **33**), the order of potency of the analogues with different R substituents (ethyl ≅ *i*-propyl > *n*-propyl) is in agreement with the length of the groups as measured by the Verloop's parameter *L*:[19] 4.11, 4.11, and 4.92, respectively.

To illustrate the SAR of the class, the binding mode of the most active compound of the series was investigated by building a three-dimensional model of the quaternary complex formed between compound **8** and AChE. The coordinates of the protein were taken from the crystal structure of *T. californica* AChE determined by Sussman et al.,[6] and a slight modification was introduced, according to the primary sequence of human AChE.[20] The identity of the active site residues of the two enzymes was carefully checked, and Phe330 was replaced by Tyr, which is present in the human AChE. The inhibitor was then docked into the active site by attaching it to the Ser200 Oγ in such a way as to

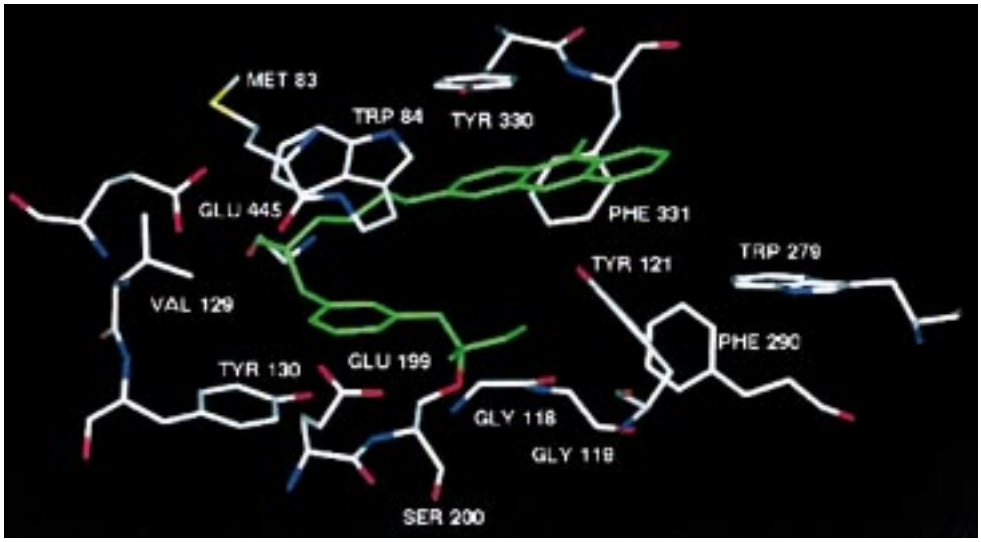

Figure 1. Inhibitor **8** (green) docked into the AChE active site gorge. Only a few amino acid residues are shown for simplicity.

represent the tetrahedral intermediate of the carbamoylation reaction, and subsequently, a molecular dynamics simulation was carried out on the complex.

The results of the simulations are shown in Figure 1, which illustrates the main features of the interactions between some AChE active site residues and compound **8**. The inhibitor (green) appears to be located in the active site gorge so as to maximize the favorable contacts, which might be the cause of its high potency. The molecule is folded, and the xanthenonyl moiety points toward the opening of the gorge, being caged within a framework of aromatic residues. From inspection of the model, it results that compound **8** (bearing an intermediate methylene chain of three carbon units) can interact with Trp84, but its tricyclic ring is not able to reach Trp279; the two mentioned residues have recently been postulated to correspond to HBS-1 and HBS-2, respectively.[21]

A more detailed description of the binding interactions of compound **8** with the AChE active site gorge is given in Figure 2.

Residues stabilizing the tetrahedral intermediate group resulting from the nucleophilic attack of Ser200 onto the carbamoyl C═O are shown in Figure 2a. The amide nitrogen atoms of Gly118 and Gly119 are hydrogen bonded to the oxyanion of the inhibitor, and the methyl substituent on the carbamic nitrogen occupies a lipophilic pocket formed mainly by Phe288, Phe290, and Phe331.

In Figure 2b, residues possibly interacting with the protonated amine group are shown. The proton is in a position favorable for establishing a hydrogen bond with the carbonyl of Gly441. The positive charge, which is distributed over the methyl or methylene groups attached to the basic N, can be stabilized by the carboxylates of Glu199 and Glu445 and by the aromatic ring of Trp84. The methyl substituent on the nitrogen interacts with a lipophilic pocket determined by Met83, Val129, and Tyr130 (Figure 1), which appears to be large enough to contain small symmetrical alkyl groups such as methyl, ethyl, and *i*-propyl.

The interactions of the xanthenonyl moiety of **8** with the binding site are illustrated in Figure 2c. Compounds containing this fragment are comparatively more potent than the corresponding derivatives bearing different heterocyclic groups (Table 2). This might be a consequence of a number of factors, like the optimal fit in the lipophilic active site gorge and some favorable interactions with specific residues. In the vicinity of the xanthenonyl nucleus, there are eight aromatic residues, some of which are shown in Figure 1. Moreover, the arrangement of the phenyl ring of Tyr330 is optimal for a stacking interaction with one benzene ring of the tricycle (the distance between the centers of the two rings is 3.44 Å), and the OH group of Tyr121 can form a hydrogen bond with the ethereal O atom of the xanthenonyl fragment (Figure 2c). On the other hand, the Phe331 side chain, which is at a suitable distance for a T-shaped interaction with the xanthone counterpart (ca. 5 Å),[22] does not show an ideal geometry.

Enzymatic Selectivity. Compounds displaying an inhibitory activity similar to or better than that of physostigmine were also tested for their inhibitory activity on isolated BuChE. The ratio between the IC_{50} value for BuChE and that for AChE is positively correlated with the specificity of the inhibitory effect on AChE. The results are summarized in Table 2, and they indicate that all the tested compounds, with the exception of compound **16**, are more active on AChE than on BuChE, the most selective being **8**, **6**, **12**, and **13**.

Unlike the inhibitory activity, AChE selectivity does not seem to be strictly related to the carbon chain length (*n*) separating the xanthenonyloxy moiety from the benzylaminic nitrogen. Compounds **8** and **6**, with a three- and a five-carbon chain length, respectively, are both highly selective. Enzymatic selectivity is affected by the size of the carbamoyl substituents (R_1) with an order of potency (methyl (**8**) > phenyl (**12**) > ethyl (**9**)) that is reflective of the order found for AChE inhibitory activity. Moreover, replacement of the methyl group on the nitrogen of the benzylaminic moiety with an ethyl group decreases the selectivity (compound **25**). The xanthenonyloxy moiety confers the best selectivity to the molecule. When the xanthone nucleus is replaced by the bioisoster azaxanthone, the selectivity is decreased, though still high (compound **13**). Selectivity is reduced to modest levels or even inverted when the

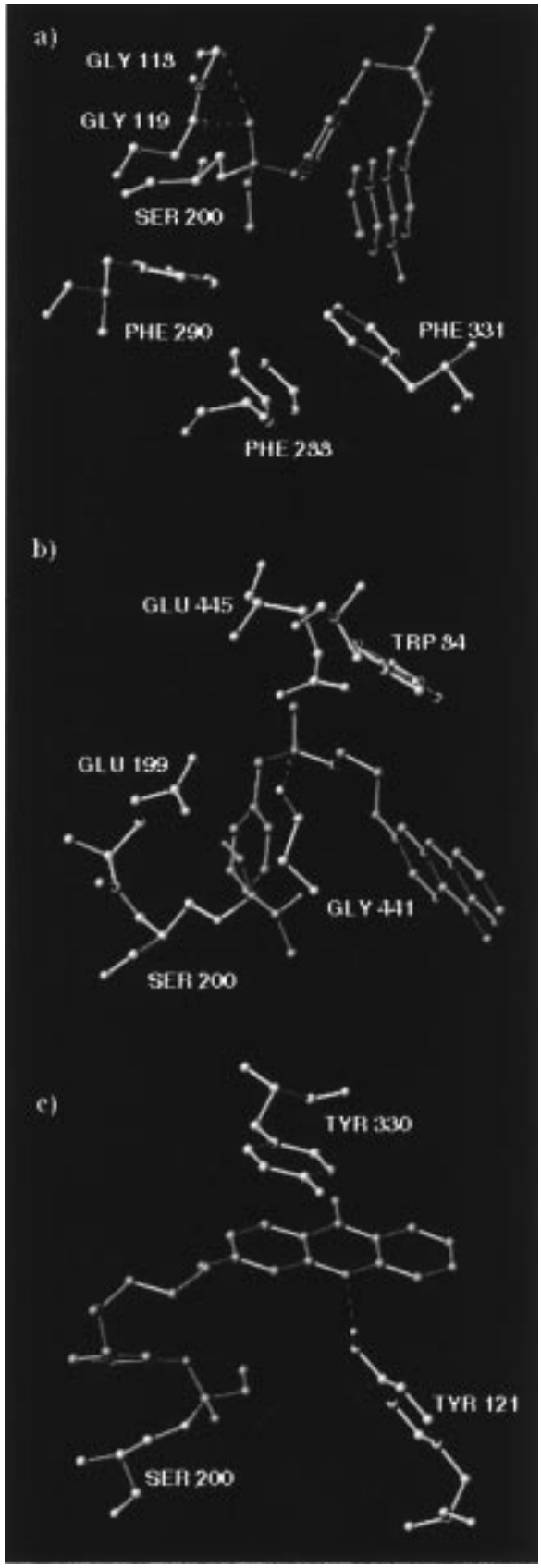

Figure 2. Detailed view of the putative binding interactions of **8** (dark) with some active site residues (light); H-bonds are shown as dashed lines. (a) Residues involved in the binding of the tetrahedral complex between Ser200 Oγ and the carbamic group. (b) Residues involved in the binding of the protonated amine group. (c) Residues involved in the binding of the xanthenonyloxy moiety.

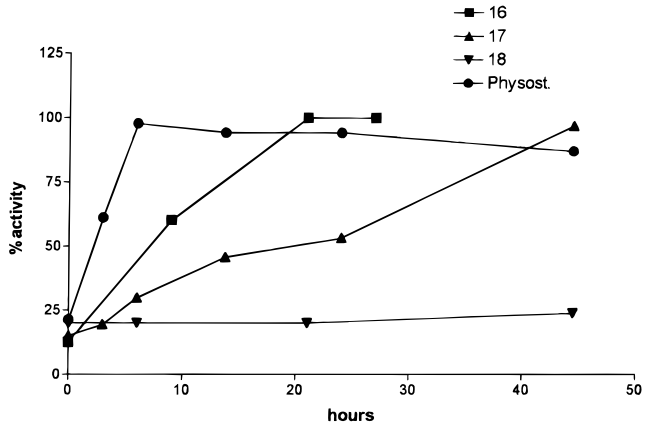

Figure 3. Progressive recovery of AChE activity after incubation with inhibitors **16**−**18**.

heterocycle is a coumarin or a flavone (compounds **18**, **22**, and **16**).

Reversibility of the Enzymatic Inhibition. As previously reported,[23] the inhibition of AChE by carbamates involves a reversible complex formation followed by carbamoylation of the hydroxyl of the catalytic serine. To study the influence of the alkyl chain length of the compounds under study on the extent of inhibition, the decarbamoylation reaction was studied for three derivatives (**16**−**18**) bearing a methyl, *n*-butyl, and *n*-heptyl substituent on the carbamic moiety, respectively. The formation of the covalent bond was confirmed by the time dependence of inhibition showed by the tested compounds. The enzyme inactivation was found to increase with the inhibitor concentration and with the enzyme−inhibitor time of incubation up to nearly 20 min for the longer chain derivatives, slightly less for the *N*-methyl-substituted derivative (**16**) at the 80% inhibition concentration.

The carbamoylated enzyme is then hydrolyzed to regenerate the free enzyme. The velocity of this step was found to be dependent on the length of the alkyl chain on the carbamate group, as previously reported for physostigmine derivatives;[4c] in particular, carbamates substituted with a longer alkyl group were found long-acting.

The results of the decarbamoylation kinetics experiments are shown in Figure 3. From the graph, it appears that the physostigmine-inhibited enzyme recovered its activity after 6 h, while in the cases of the coumarin derivatives **16**−**18**, the recovery times were much longer. Actually, the enzyme inhibited with compound **16** recovered its activity after 21 h, compound **17** after 44 h, and the *n*-heptyl derivative **18** was still inhibited after 48 h.

To verify the reversibility of action also for the long-acting compound **18**, the heptylcarbamoylated enzyme was isolated after 48 h dialysis and, after dilution, its hydrolysis was followed to determine the decarbamoylation rate constant.[23a] Under the described experimental conditions, it was possible to follow the recovery of the enzyme activity (up to 40%). During the experiment, the stability of the reference enzyme was also checked: the activity was maintained after the dialysis and a 15% loss of activity was observed after the dilution. The decarbamoylation rate constant k_3 (5.05×10^{-3} min^{-1}) is the slope of the linear plot ($r^2 = 0.9780$) calculated as described in the Experimental Section.

In Vitro Inhibition of AChE Activity in Rat Cerebral Cortex. The AChE inhibitory activity of some of the most interesting compounds of the present series was tested in AChE-enriched preparations obtained from partial fractionation of rat brain cortex homogenates (see Experimental Section). The results are shown in Table 2, and they indicate that, while most of the SAR established with the purified enzyme assays still hold, some significant differences are seen for specific compounds. As found with the isolated enzyme, a good inhibitory activity requires a three-carbon chain length separating the xanthenonyloxy moiety from the benzylaminic nitrogen (compounds **8** and **9**). The activity decreases with the size of the carbamoyl substituents (R_1), but opposite to what is found when using the purified enzyme, the phenyl substitution leads to a dramatic loss of activity (compound **12**). Variation of the heteroaryloxy moiety (Ar) leads to a ranking of activities, which is strikingly different from that obtained with isolated AChE, with the xanthone moiety being the least active (compound **8**). Replacing the xanthone nucleus with the bioisoster azaxanthone (compound **13**) greatly enhances the inhibitory activity, followed by the flavone (compound **22**) and the coumarin (compound **16**) substitutions. With regard to the amine substituent (R), the inhibitory activity is slightly higher with the ethyl group (compound **25**) than with the methyl group (compound **8**).

In these experimental conditions, the inhibitory activity of physostigmine is higher than that found for the purified enzyme. As a result, the only compounds which are still more active than physostigmine are those with modifications in the heteroaryloxy moiety and namely **13**, **16**, and **22**.

Inhibition experiments conducted in the presence of a saturating concentration of acetylcholine (2 mM) resulted in higher IC_{50} values for the compounds (data not shown), an underestimation expected when working with competitive inhibitors.[24]

Discussion

The AChE inhibitory activity of a series of xanthone carbamoyloxy derivatives was examined. Four different parts of the molecule were modified and analyzed for determining the structure−activity relationships, using both isolated AChE and rat cerebral cortex AChE. Enzymatic selectivity was determined comparing the inhibitory activity of the compounds on BuChE with that exerted on AChE. Reversibility of the inhibition was also verified.

Several structural clues have been highlighted from this study with regard to the AChE inhibition:

(a) In accordance with earlier reports,[9] optimum inhibitory activity requires a three-carbon-atom chain separating the heteroaryloxy moiety from the basic nitrogen. In light of the model of Figure 1, one can note that the length of the intermediate methylene chain is critical in influencing the position of the heterocyclic moiety and, consequently, in allowing the very specific interactions responsible for the global high affinity to the enzyme. Increasing *n* of one carbon unit might disrupt the optimal array of contacts, while lengthening the chain up to five C units might reconstitute the framework or compensate for the lost interactions with new ones. On the other hand, the linker chain does not seem to be responsible for the enzymatic selectivity.

(b) A small size of the carbamic substituent is critical for both inhibitory potency and enzymatic selectivity. Both parameters are best when the substituent is a methyl group. The loss of activity occurring with larger alkyl groups is most likely due to a bad fitting of this part of the molecule in a small lipophilic pocket of the enzyme (the AChE esteratic site). On the other hand, the rate of enzyme regeneration is inversely correlated with the length of the alkyl substituent, even if interesting results can also be obtained with a methyl group. In fact, the complex formed between AChE and compound **16** has a much longer stability than that formed by physostigmine, and the duration of action increases dramatically by increasing the chain length. The longer recovery time of the former complex with respect to that of the enzyme−physostigmine complex might be due to different residual affinities of the hydrolyzed moieties. The benzylaminic fragment of **16** might contribute to the longer lasting inhibition, having a higher affinity for the enzyme than the eseroline fragment of physostigmine.

(c) The inhibitory activity requires the presence of a methyl group on the basic nitrogen. Slightly larger substituents (up to *i*-propyl) are tolerated without seriously decreasing activity because they can occupy a hydrophobic cavity lined by the residues Met83, Val129, and Tyr130 (see Figure 1).

(d) Replacement of the xanthone moiety of the lead molecule **8** with either the bioisoster azaxanthone or the analogues coumarin or flavone reduces in most cases both the inhibitory activity on isolated enzyme and the selectivity. This might be a consequence of the relative stereoelectronic dissimilarity of the former heteroaryloxy groups with respect to the xanthone parent structure. However, the working hypothesis at the basis of the modifications still seems valid, as the activity is maintained at quite acceptable levels.

When tested on the rat cerebral cortex AChE, the order of potency of the various heteroaryloxy-substituted compounds is totally different from that noticed with the isolated enzyme, and the azaxanthone derivative (compound **13**) is the most active. This difference might be related to the steric complexity of biological environment, which can cause structural changes in the conformation of enzymes with respect to the native form of the isolated protein. Moreover, tissue-bound enzymatic activities can affect the chemical structure of drugs, making them more or less available for the enzyme to inhibit. If present, such differences between the isolated and the tissue-bound preparations can affect the enzymatic activities as well as sensitivities to modulating drugs. AChE can indeed be present in different molecular forms. Such forms are known to exhibit virtually the same enzymatic activity; however, a contribution to the inhibitory potencies of the compounds examined cannot be ruled out.

Conclusions

In conclusion, this study led to the identification of a series of compounds showing an inhibitory potency on AChE up to the subnanomolar level. The enzyme−inhibitor binding mode and the structure−activity

relationships were determined, and a detailed investigation of the biological properties was carried out. One derivative was identified as possessing all the structural requirements established for best activity and selectivity for AChE inhibition. This molecule is compound **13**, an azaxanthone derivative 190-fold more potent than physostigmine on rat brain AChE and over 60-fold more selective for AChE than for BuChE. This compound has thus been selected for further development.

Experimental Section

Chemistry. General Methods. All melting points were determined in open glass capillaries using a Büchi apparatus and are uncorrected. ^{1}H NMR spectra were recorded in $CDCl_3$ solution on a Varian Gemini 300 spectrometer with Me_4Si as the internal standard. Wherever analyses are only indicated with element symbols, analytical results obtained for those elements are within 0.4% of the theoretical values.

3-(5-Chloropentoxy)xanthen-9-one (1c). A stirred suspension of 2.12 g (0.01 mol) of 3-hydroxyxanthen-9-one, 1.85 g (0.01 mol) of 1-bromo-5-chloropentane, and 1.4 g (0.01 mol) of K_2CO_3 in dry acetone was refluxed for 24 h. The reaction was monitored by TLC. The hot reaction mixture was filtered and evaporated to dryness. The residue was crystallized from toluene to give 2.2 g (70%) of **1c**: mp 128−130 °C (EtOH); ^{1}H NMR δ 1.7 (m, 2H), 1.9 (m, 4H), 3.6 (t, 2H), 4.1 (t, 2H), 6.85−8.4 (m, 7H, Ar). Anal. ($C_{18}H_{17}ClO_3$): C, H.

3-(3-Chloropropoxy)-5-azaxanthen-9-one (1d). Using the previous procedure and starting from 2.13 g (0.01 mol) of 3-hydroxy-5-azaxanthen-9-one and 1.57 g (0.01 mol) of 1-bromo-3-chloropropane, 2.1 g (70%) of **1d** was obtained: mp 174−175 °C (toluene); ^{1}H NMR (DMSO-d_6) δ 2.25 (m, 2H), 3.85 (t, 2H), 4.3 (t, 2H), 7.1−8.8 (m, 6H, Ar). Anal. ($C_{15}H_{12}ClNO_3$): C, H, N.

7-(3-Chloropropoxy)-2*H*-1-benzopyran-2-one (1e). Using the previous procedure and starting from 1.62 g (0.01 mol) of 7-hydroxy-2*H*-1-benzopyran-2-one, 1.78 g (75%) of **1e** was obtained: mp 105−108 °C (toluene); ^{1}H NMR δ 2.3 (m, 2H), 3.75 (t, 2H), 4.2 (t, 2H), 6.25 (d, 1H, H-3), 6.8−7.4 (m, 3H, Ar), 7.65 (d, 1H, H-4). Anal. ($C_{12}H_{11}ClO_3$): C, H.

7-(3-Chloropropoxy)-4*H*-1-benzopyran-4-one (1f). Using the previous procedure and starting from 1.62 g (0.01 mol) of 7-hydroxy-4*H*-1-benzopyran-4-one, 2.14 g (90%) of **1f** was obtained: mp 73−75 °C (ligroin); ^{1}H NMR δ 2.3 (m, 2H), 3.75 (t, 2H), 4.2 (t, 2H), 5.8 (d, 1H, H-2), 6.4−7.7 (m, 3H, Ar), 8.1 (d, 1H, H-3). Anal. ($C_{12}H_{11}ClO_3$): C, H.

7-(3-Chloropropoxy)-2-phenyl-4*H*-1-benzopyran-4-one (1g). Using the previous procedure and starting from 2.38 g (0.01 mol) of 7-hydroxy-4*H*-1-benzopyran-4-one, 2.2 g (70%) of **1g** was obtained: mp 118−121 °C (toluene); ^{1}H NMR δ 2.35 (m, 2H), 3.8 (t, 2H), 4.25 (t, 2H), 6.8−8.2 (m, 9H, Ar and H-3). Anal. ($C_{18}H_{15}ClO_3$): C, H.

3-(3-Iodopropoxy)xanthen-9-one (2a). A mixture of 2.88 g (0.01 mol) of 3-(3-chloropropoxy)-xanthen-9-one[9] and 1.5 g (0.01 mol) of NaI in 30 mL of methyl ethyl ketone was refluxed for 4 h. After cooling, the separated solid was collected by filtration and 2.66 g (70%) of **2a** was obtained: mp 119−121 °C; ^{1}H NMR δ 2.35 (m, 2H), 3.45 (t, 2H), 4.3 (t, 2H), 6.9−8.4 (m, 7H, Ar). Anal. ($C_{16}H_{13}IO_3$): C, H.

3-(4-Iodobutoxy)xanthen-9-one (2b). Using the previous procedure and starting from 3 g (0.01 mol) of 3-(4-chlorobutoxy)xanthen-9-one,[9] 2.76 g (70%) of **2b** was obtained: mp 113−115 °C; ^{1}H NMR δ 2.05 (m, 4H), 3.3 (t, 2H), 4.15 (t, 2H), 6.85−8.4 (m, 7H, Ar). Anal. ($C_{17}H_{15}IO_3$): C, H.

3-(5-Iodopentoxy)xanthen-9-one (2c). Using the previous procedure and starting from 3.16 g (0.01 mol) of **1c**, 3.3 g (80%) of **2c** was obtained: mp 129−131 °C; ^{1}H NMR δ 1.7 (m, 2H), 1.9 (m, 4H), 3.3 (t, 2H), 4.15 (t, 2H), 6.85−8.4 (m, 7H, Ar). Anal. ($C_{18}H_{17}IO_3$): C, H.

3-(3-Iodopropoxy)-5-azaxanthen-9-one (2d). Using the previous procedure and starting from 2.89 g (0.01 mol) of **1d**, 3 g (80%) of **2d** was obtained: mp 165−166 °C; ^{1}H NMR δ (DMSO-d_6) 2.25 (m, 2H), 3.45 (t, 2H), 4.2 (t, 2H), 7.1−8.8 (m, 6H, Ar). Anal. ($C_{15}H_{12}INO_3$): C, H, N.

7-(3-Iodopropoxy)-2*H*-1-benzopyran-2-one (2e). Using the previous procedure and starting from 2.38 g (0.01 mol) of **1e**, 2.5 g (75%) of **2e** was obtained: mp 98−100 °C; ^{1}H NMR δ 2.3 (m, 2H), 3.35 (t, 2H), 4.1 (t, 2H), 6.25 (d, 1H, H-3), 6.8−7.4 (m, 3H, Ar), 7.65 (d, 1H, H-4). Anal. ($C_{12}H_{11}IO_3$): C, H.

7-(3-Iodopropoxy)-4*H*-1-benzopyran-4-one (2f). Using the previous procedure and starting from 2.38 g (0.01 mol) of **1f**, 3 g (90%) of **2f** was obtained: mp 121−122 °C; ^{1}H NMR δ 2.3 (m, 2H), 3.35 (t, 2H), 4.1 (t, 2H), 5.8 (d, 1H, H-2), 6.4−7.7 (m, 3H, Ar), 8.1 (d, 1H, H-3). Anal. ($C_{12}H_{11}IO_3$): C, H.

7-(3-Iodopropoxy)-2-phenyl-4*H*-1-benzopyran-4-one (2g). Using the previous procedure and starting from 3.14 g (0.01 mol) of **1g**, 3.25 g (80%) of **2g** was obtained: mp 131−133 °C; ^{1}H NMR δ 2.35 (m, 2H), 3.4 (t, 2H), 4.2 (t, 2H), 6.8−8.2 (m, 9H, Ar and H-3). Anal. ($C_{18}H_{15}IO_3$): C, H.

3-[*N*-Methyl-*N*-(3-hydroxybenzyl)amino]propoxyxanthen-9-one (3a). A solution of 1.9 g (0.005 mol) of **2a** and 1.37 g (0.01 mol) of *N*-(3-hydroxybenzyl)methylamine in 100 mL of toluene was refluxed for 15 h. After cooling, the reaction mixture was washed (H_2O), dried (Na_2SO_4), and evaporated to dryness. The residue, on crystallizing from toluene, afforded 1.13 g (60%) of **3a**: mp 148−150 °C; ^{1}H NMR δ 2.05 (m, 2H), 2.3 (s, 3H), 2.6 (t, 2H), 3.5 (s, 2H), 4.15 (t, 2H), 6.7−8.4 (m, 11H, Ar). Anal. ($C_{24}H_{23}NO_4$): C, H, N.

3-[*N*-Methyl-*N*-(3-hydroxybenzyl)amino]butoxyxanthen-9-one (3b). Using the previous procedure and starting from 0.98 g (0.0025 mol) of **2b**, 0.6 g (60%) of **3b** was obtained: mp 96−98 °C (toluene); ^{1}H NMR δ 1.7−1.9 (m, 4H), 2.25 (s, 3H), 2.5 (t, 2H), 3.5 (s, 2H), 4.05 (t, 2H), 6.7−8.4 (m, 11H, Ar). Anal. ($C_{25}H_{25}NO_4$): C, H, N.

3-[*N*-Methyl-*N*-(3-hydroxybenzyl)amino]pentoxyxanthen-9-one (3c). Using the previous procedure and starting from 3.22 g (0.0064 mol) of **2c**, 1.35 g (50%) of **3c** was obtained: mp 101−103 °C (toluene); ^{1}H NMR δ 1.4−1.65 (m, 4H), 1.8 (m, 2H), 2.2 (s, 3H), 2.4 (t, 2H), 3.45 (s, 2H), 4.05 (t, 2H), 6.7−8.4 (m, 11H, Ar). Anal. ($C_{26}H_{27}NO_4$): C, H, N.

3-[*N*-Methyl-*N*-(3-hydroxybenzyl)amino]propoxy-5-azaxanthen-9-one (3d). Using the previous procedure and starting from 1.9 g (0.005 mol) of **2d**, 1.17 g (60%) of **3d** was obtained: mp 162−164 °C (toluene); ^{1}H NMR δ 2.0 (m, 2H), 2.2 (s, 3H), 2.5 (t, 2H), 3.4 (s, 2H), 4.15 (t, 2H), 6.7−8.7 (m, 10H, Ar). Anal. ($C_{23}H_{22}N_2O_4$): C, H, N.

7-[*N*-Methyl-*N*-(3-hydroxybenzyl)amino]propoxy-2*H*-1-benzopyran-2-one (3e). Using the previous procedure and starting from 1.65 g (0.005 mol) of **2e**, 1.19 g (70%) of **3e** was obtained: mp 90−92 °C (toluene); ^{1}H NMR δ 2.0 (m, 2H), 2.23 (s, 3H), 2.55 (t, 2H), 3.45 (s, 2H), 4.1 (t, 2H), 6.25 (d, 1H, H-3), 6.7−7.75 (m, 8H, Ar and H-4). Anal. ($C_{20}H_{21}NO_4$): C, H, N.

7-[*N*-Methyl-*N*-(3-hydroxybenzyl)amino]propoxy-4*H*-1-benzopyran-4-one (3f). Using the previous procedure and starting from 1.65 g (0.005 mol) of **2f**, 0.85 g (50%) of **3f** was obtained: mp 62−65 °C (toluene); ^{1}H NMR δ 2.0 (m, 2H), 2.25 (s, 3H), 2.55 (t, 2H), 3.5 (s, 2H), 4.0 (t, 2H), 5.8 (d, 1H, H-2), 6.3−8.15 (m, 8H, Ar and H-3). Anal. ($C_{20}H_{21}NO_4$): C, H, N.

7-[*N*-Methyl-*N*-(3-hydroxybenzyl)amino]propoxy-2-phenyl-4*H*-1-benzopyran-4-one (3g). Using the previous procedure and starting from 2.03 g (0.005 mol) of **2g**, 1.04 g (50%) of **3g** was obtained: mp 117−118 °C (toluene); ^{1}H NMR δ 2.0 (m, 2H), 2.25 (s, 3H), 2.55 (t, 2H), 3.5 (s, 2H), 4.1 (t, 2H), 6.7−8.1 (m, 13H, Ar and H-3). Anal. ($C_{26}H_{25}NO_4$): C, H, N.

3-[*N*-Ethyl-*N*-(3-hydroxybenzyl)amino]propoxyxanthen-9-one (3h). Using the previous procedure and starting from 2.5 g (0.0065 mol) of **2a** and 2 g (0.013 mol) of *N*-(3-hydroxybenzyl)ethylamine, 1.53 g (70%) of **3h** was obtained: mp 206−208 °C (toluene); ^{1}H NMR δ 1.1 (t, 3H), 2.0 (m, 2H), 2.5−2.7 (m, 4H), 3.55 (s, 2H), 4.1 (t, 2H), 6.65−8.35 (m, 11H, Ar). Anal. ($C_{25}H_{25}NO_4$): C, H, N.

3-[*N*-*n*-Propyl-*N*-(3-hydroxybenzyl)amino]propoxyxanthen-9-one (3i). Using the previous procedure and starting from 2 g (0.005 mol) of **2a** and 1.6 g (0.01 mol) of *N*-(3-hydroxybenzyl)-*n*-propylamine, 1.04 g (50%) of **3i** was obtained: mp 142−144 °C (toluene); ^{1}H NMR δ 0.8 (t, 3H), 1.8 (m, 2H),

2.3 (m, 2H), 2.75 (m, 2H), 3.05 (m, 2H), 3.9−4.1 (m, 4H), 6.7−8.2 (m, 11H, Ar). Anal. ($C_{26}H_{27}NO_4$): C, H, N.

3-[*N*-Isopropyl-*N*-(3-hydroxybenzyl)amino]propoxyxanthen-9-one (3j). Using the previous procedure and starting from 2 g (0.005 mol) of **2a** and 1.6 g (0.01 mol) of *N*-(3-hydroxybenzyl)-isopropylamine, 1.25 g (60%) of **3j** was obtained: mp 122−124 °C (toluene); ^{1}H NMR δ 1.0 (s, 3H), 1.05 (s, 3H), 1.9 (m, 2H), 2.65 (t, 2H), 2.95 (m, 1H), 3.55 (s, 2H), 4.1 (t, 2H), 6.65−8.35 (m, 11H, Ar). Anal. ($C_{26}H_{27}NO_4$): C, H, N.

General Method for the Preparation of Carbamates (4−33). A mixture of the selected ω-[*N*-alkyl-*N*-(3-hydroxy)-benzyl]aminoalkoxy derivative (0.001 mol), selected alkyl isocyanate (0.001 mol), and 10 mg of sodium hydride in toluene was stirred at room temperature for 24 h, quenched with water, and then extracted with methylene chloride. The organic layer was washed with water, dried and evaporated to dryness. The residue was purified by crystallization or by flash chromatography.

^{1}H NMR for Compounds 4−33. 4: δ (DMSO-d_6) 1.7−1.9 (m, 4H), 2.6 (s, 3H), 2.7 (d, 3H), 3.0 (m, 2H), 4.05−4.4 (m, 4H), 6.9−8.25 (m, 11H, Ar). **5**: δ (DMSO-d_6) 0.85 (t, 3H), 1.2 (m, 8H), 1.4 (m, 2H), 1.7−1.9 (m, 4H), 2.65 (s, 3H), 2.9−3.2 (m, 4H), 4.1−4.4 (m, 4H), 7.0−8.2 (m, 12 H, Ar and NH). **6**: δ ($CDCl_3$) 1.4−1.65 (m, 4H), 1.85 (m, 2H), 2.2 (s, 3H), 2.4 (t, 2H), 2.85 (d, 3H), 3.45 (s, 2H), 4.05 (t, 2H), 4.95 (broad, 1H, NH), 6.8−8.4 (m, 11H, Ar). **7**: δ (DMSO-d_6) 0.8 (t, 3H), 1.25 (m, 8H), 1.45 (m, 4H), 1.8 (m, 4H), 2.65 (s, 3H), 2.9−3.2 (m, 4H), 4.1−4.4 (m, 4H), 7.0−8.2 (m, 12H, Ar and NH). **8**: δ ($CDCl_3$) 2.0 (m, 2H), 2.25 (s, 3H), 2.55 (t, 2H), 2.85 (d, 3H), 3.5 (s, 2H), 4.15 (t, 2H), 4.95 (broad, 1H, NH), 6.8−8.4 (m, 11H, Ar). **9**: δ ($CDCl_3$) 1.2 (t, 3H), 2.05 (m, 2H), 2.3 (s, 3H), 2.6 (t, 2H), 3.3 (m, 2H), 3.55 (s, 2H), 4.2 (t, 2H), 5.0 (broad, 1H, NH), 6.9−8.4 (m, 11H, Ar). **10**: δ ($CDCl_3$) 0.95 (t, 3H), 1.6 (m, 2H), 2.05 (m, 2H), 2.3 (s, 3H), 2.6 (t, 2H), 3.2 (m, 2H), 3.55 (s, 2H), 4.2 (t, 2H), 5.0 (broad, 1H, NH), 6.85−8.4 (m, 11H, Ar). **11**: δ ($CDCl_3$) 0.95 (t, 3H), 1.35 (m, 2H), 1.5 (m, 2H), 2.05 (m, 2H), 2.3 (s, 3H), 2.6 (t, 2H), 3.2 (m, 2H), 3.55 (s, 2H), 4.15 (t, 2H), 5.05 (broad, 1H, NH), 6.85−8.4 (m, 11H, Ar). **12**: δ (DMSO-d_6) 2.3 (m, 2H), 2.7 (s, 3H), 3.2 (m, 2H), 4.2−4.5 (m, 4H), 7.0−8.2 (m, 16H, Ar), 10.32 (s, 1H, NH). **13**: δ (DMSO-d_6) 2.25 (m, 2H), 2.6−2.75 (m, 6H), 3.15 (m, 2H), 4.2−4.5 (m, 4H), 7.0−8.8 (m, 10H, Ar). **14**: δ (DMSO-d_6) 0.85 (t, 3H), 1.25−1.5 (m, 4H), 2.3 (m, 2H), 3.7 (s, 3H), 3.05 (m, 2H), 3.2 (m, 2H), 4.2−4.5 (m, 4H), 7.0−8.8 (m, 11H, Ar and NH). **15**: δ (DMSO-d_6) 0.85 (t, 3H), 1.25 (m, 8H), 1.45 (m, 2H), 2.25 (m, 2H), 2.7 (s, 3H), 3.0 (m, 2H), 3.2 (m, 2H), 4.2−4.5 (m, 4H), 7.0−8.8 (m, 11H, Ar and NH). **16**: δ (DMSO-d_6) 2.25 (m, 2H), 2.6 (s, 3H), 2.65 (s, 3H), 3.2 (m, 2H), 4.1−4.5 (m, 4H), 6.3 (d, 1H), 6.9−8.05 (m, 8H, Ar and H-4 coumarin). **17**: δ ($CDCl_3$) 0.95 (t, 3H), 1.4 (m, 2H), 1.6 (m, 2H), 2.0 (m, 2H), 2.25 (s, 3H), 2.5 (t, 2H), 3.3 (m, 2H), 3.5 (s, 2H), 4.05 (t, 2H), 5.25 (broad, 1H, NH), 6.25 (d, 1H), 6.8−7.2 (m, 8H, Ar and 4-H coumarin). **18**: δ (DMSO-d_6) 0.8 (t, 3H), 1.25 (m, 8H), 1.4 (m, 2H), 2.25 (m, 2H), 2.65 (s, 3H), 3.0 (m, 2H), 3.2 (m, 2H), 4.15 (s, 2H), 4.3 (m, 2H), 6.3 (d, 1H), 6.85−8.0 (m, 9H, Ar, NH and H-4 coumarin). **19**: δ (DMSO-d_6) 2.2 (m, 2H), 2.6−2.7 (m, 6H), 3.2 (m, 2H), 4.05−4.5 (m, 4H), 6.25 (d, 1H), 7.0−8.2 (m, 8H, Ar and H-3). **20**: δ (DMSO-d_6) 0.85 (t, 3H), 1.45 (m, 2H), 2.2 (m, 2H), 2.75 (s, 3H), 3.0 (m, 2H), 3.2 (m, 2H), 4.1−4.5 (m, 4H), 6.25 (d, 1H), 6.9−8.2 (m, 9H, Ar, NH and H-3). **21**: δ (DMSO-d_6) 0.85 (t, 3H), 1.25 (m, 8H), 1.5 (m, 2H), 2.25 (m, 2H), 2.7 (s, 3H), 3.05 (m, 2H), 3.2 (m, 2H), 4.1−4.5 (m, 4H), 6.3 (d, 1H), 7.0−8.2 (m, 9H, Ar, NH and H-3). **22**: δ (DMSO-d_6) 2.3 (m, 2H), 2.6−2.75 (m, 6H), 3.2 (m, 2H), 4.1−4.5 (m, 4H), 6.95−8.15 (m, 13H, Ar and H-3). **23**: δ (DMSO-d_6) 0.85 (t, 3H), 1.2−1.5 (m, 4H), 2.3 (m, 2H), 2.7 (s, 3H), 3.0 (m, 2H), 3.2 (m, 2H), 4.15−4.5 (m, 4H), 6.9−8.1 (m, 14 H, Ar, NH and H-3). **24**: δ (DMSO-d_6) 0.8 (t, 3H), 1.2 (m, 8H), 1.4 (m, 2H), 2.25 (m, 2H), 2.7 (s, 3H), 3.0 (m, 2H), 3.2 (m, 2H), 4.15−4.5 (m, 4H), 6.95−8.1 (m, 14H, Ar, NH and H-3). **25**: δ ($CDCl_3$) 1.05 (t, 3H), 1.95 (m, 2H), 2.5−2.7 (m, 4H), 2.85 (d, 3H), 3.55 (s, 2H), 4.1 (t, 2H), 4.95 (broad, 1H, NH), 6.8−8.4 (m, 11H, Ar). **26**: δ ($CDCl_3$) 0.9 (t, 3H), 1.1 (t, 3H), 1.35 (m, 2H), 1.5 (m, 2H), 1.95 (m, 2H), 2.5−2.7 (m, 4H), 3.2 (m, 2H), 3.6 (s, 2H), 4.1 (t, 2H), 4.95 (broad, 1H, NH), 6.8−8.4 (m, 11H, Ar). **27**: δ (DMSO-d_6) 0.8 (t, 3H), 1.1−1.3 (m, 11H), 1.4 (m, 2H), 2.2 (m, 2H), 2.95−3.4 (m, 6H), 4.1−4.4 (m, 4H), 6.95−8.2 (m, 12H, Ar and NH). **28**: δ (DMSO-d_6) 0.9 (t, 3H), 1.8 (m, 2H), 2.3 (m, 2H), 2.7 (d, 3H), 3.05 (m, 2H), 3.25 (m, 2H), 4.25 (s, 2H), 4.2−4.5 (m, 4H), 7.0−8.2 (m, 12H, Ar and NH). **29**: δ (DMSO-d_6) 0.9 (m, 6H), 1.3 (m, 2H), 1.45 (m, 2H), 1.75 (m, 2H), 2.25 (m, 2H), 3.05 (m, 4H), 3.25 (m, 2H), 4.2−4.5 (m, 4H), 7.0−8.2 (m, 12H, Ar and NH). **30**: δ (DMSO-d_6) 0.85 (m, 6H), 1.2 (m, 8H), 1.4 (m, 2H), 1.75 (m, 2H), 2.25 (m, 2H), 3.05 (m, 4H), 3.25 (m, 2H), 4.2−4.4 (m, 4H), 7.0−8.2 (m, 12H, Ar and NH). **31**: δ ($CDCl_3$) 1.0 (d, 6H), 1.9 (m, 2H), 2.6 (t, 2H), 2.85 (d, 3H), 2.95 (m, 2H), 3.55 (s, 2H), 4.1 (t, 2H), 4.95 (broad,1H, NH), 6.8−8.4 (m, 11H, Ar). **32**: δ ($CDCl_3$) 0.9 (t, 3H), 1.0 (d, 6H), 1.35 (m, 2H), 1.55 (m, 2H), 1.9 (m, 2H), 2.65 (t, 2H), 3.0 (m, 1H), 3.25 (m, 2H), 3.6 (s, 2H), 4.1 (t, 2H), 5.0 (broad, 1H, NH), 6.8−8.4 (m, 11H, Ar). **33**: δ (DMSO-d_6) 0.8 (t, 3H), 1.2 (m, 8H), 1.35 (d, 6H), 2.2 (m, 2H), 2.95−3.25 (m, 4H), 3.6 (m, 1H), 4.1−4.5 (m, 4H), 6.95−8.2 (m, 12H, Ar and NH).

***N*-Methyl-*N*-[(3-hydroxyphenyl)methyl]imine.** Methylamine solution (30%, 3 mL) was added rapidly to a solution of 3-hydroxybenzaldehyde (2 g, 0.016 mol) in ethanol (10 mL) at about 40 °C. The mixture was allowed to stand at 0−5 °C for 2 h. The resulting precipitate was collected by filtration, washed successively with 40% ethanol and water, and dried in vacuo to give the Schiff base (2.16 g, 100%): mp 157−159 °C; ^{1}H NMR δ 3.4 (d, 3H), 6.8−7.3 (m, 4H), 7.85 (d, 1H).

***N*-Ethyl-*N*-[(3-hydroxyphenyl)methyl]imine.** Using the previous procedure and starting from ethylamine solution (70%, 1 mL) and 1.22 g of 3-hydroxybenzaldehyde, 1.3 g (88%) was obtained: mp 128−129 °C (lit.[8] mp 127−129 °C); ^{1}H NMR δ 1.3 (t, 3H,), 3.6 (m, 2H), 6.9−7.3 (m, 4H, 7.85 (s, 1H).

***N*-Propyl-*N*-[(3-hydroxyphenyl)methyl]imine.** A solution of *n*-propylamine (5.02 g, 0.085 mol) and 3-hydroxybenzaldehyde (10.3 g, 0.085 mol) was stirred for 1 h and then was refluxed until 90−95% of the theoretical amount of H_2O was collected in a Dean−Stark trap. After cooling, the precipitate was collected by filtration to give 11.7 g (90%) of product: mp 123−125 °C; ^{1}H NMR δ 0.9 (t, 3H), 1.7 (m, 2H), 3.55 (t, 2H), 6.9−7.4 (m, 5H), 8.1 (s, 1H).

***N*-Isopropyl-*N*-[(3-hydroxyphenyl)methyl]imine.** Using the previous procedure and starting from 10.3 g of 3-hydroxybenzaldehyde, 11.7 g (90%) of product was obtained: mp 84−86 °C (petroleum ether); ^{1}H NMR δ 1.2 (s, 3H), 1.3 (s, 3H), 3.55 (m, 1H), 6.8−7.3 (m, 4H), 7.45 (broad, 1H), 8.15 (s, 1H).

***N*-Methyl-*N*-[(3-hydroxyphenyl)methyl]amine.** Sodium borohydride (0.5 g) was added portionwise to a solution of the Schiff base (1.25 g) in ethanol (20 mL) at 0−5 °C. The mixture was stirred for 20 h and quenched with water. Ethanol was evaporated, and the remaining aqueous solution was extracted with CH_2Cl_2. The organic solution was dried over Na_2SO_4, and the solvent was evaporated. The residue was crystallized from ligroin to give 1.2 g (80%) of product: mp 112−113 °C; ^{1}H NMR δ 2.45 (s, 3H), 3.6 (s, 2H), 5.4 (broad, 1H), 6.6−7.2 (m, 4H). Anal. (C_7H_9NO): C, H, N.

***N*-Ethyl-*N*-[(3-hydroxyphenyl)methyl]amine.** Using the previous procedure and starting from 1.49 g (0.01 mol) of Schiff base, 1.36 g (90%) of product was obtained: mp 106−109 °C (lit.[8] mp 107−111 °C); ^{1}H NMR δ ($CDCl_3$) 1.15 (t, 3H), 2.75 (m, 2H), 3.7 (s, 2H), 5.15 (broad, 1H), 6.6−7.2 (m, 4H).

***N*-Propyl-*N*-[(3-hydroxyphenyl)methyl]amine.** Using the previous procedure and starting from 1.63 g (0.01 mol) of Schiff base, 1.5 g (90%) of product was obtained: mp 75−77 °C; ^{1}H NMR δ 0.9 (t, 3H), 1.55 (m, 2H), 2.6 (t, 2H), 3.7 (s, 2H), 5.9 (broad, 1H), 6.6−7.2 (m, 4H). Anal. ($C_9H_{13}NO$): C, H, N.

***N*-Isopropyl-*N*-[(3-hydroxyphenyl)methyl]amine.** Using the previous procedure and starting from 1.63 g (0.01 mol) of Schiff base, 1.5 g (90%) of product was obtained: mp 128−130 °C; ^{1}H NMR δ 1.1 (s, 3H), 1.2 (s, 3H), 2.9 (m, 1H), 3.7 (s, 2H), 5.15 (broad, 1H), 6.7−7.2 (m, 4H). Anal. ($C_9H_{13}NO$): C, H, N.

Inhibition of Isolated AChE and BuChE. The method of Ellman et al.[25] was followed. The assay solution consisted of a 0.1 M phosphate buffer pH 8.0 with the addition of 340 μM 5,5′-dithio-bis(2-nitrobenzoic acid) (DTNB, Ellman's reagent), 0.035 unit/mL AChE derived from human erythrocytes (Sigma Chemical Co.), and 550 μM acetylthiocoline iodide. The final assay volume was 1 mL.

Test compounds were added to the assay solution and preincubated with the enzyme for 20 min, the addition of substrate following. The time dependence of inhibition was assessed by testing enzyme activities with inhibitor IC_{50} concentration at 5 min intervals up to 60 min of preincubation time at 37 °C. Changes in absorbances at 412 nm were recorded for 5 min, the reaction rates were compared, and the percent inhibition due to the presence of test compounds was calculated.

Inhibition of BuChE was measured as described above, substituting 0.035 unit/mL BuChE from human serum (Sigma Chemical Co.) and 550 μM butyrylthiocholine for enzyme and substrate, respectively.

Decarbamoylation Kinetics. Stock solutions in replicates were prepared as following: the free enzyme (0.65 units in 3 mL of 0.1 M phosphate buffer pH 8.0), the same amount of enzyme plus 0.9 nmol of physostigmine, and the same amount of enzyme plus 0.3 nmol of the tested inhibitors **16**, **17**, and **18**, respectively.

The solutions were gently stirred and incubated at 35 °C for 20 min. They were then loaded into 12.000 MW cutoff dialysis bags and dialyzed at 4 °C against 2 L of 0.1 M phosphate buffer pH 8.0. The dialysate was replaced four times during the first 6 h. Dialysis was interrupted after 6−12−18−24−48 h. The solutions were five times diluted with the same buffer and kept at 20−22 °C under magnetic stirring. Aliquots of 0.95 mL of each solution were sampled, and the enzyme activity was spectrophotometrically tested after addition of 0.033 mL of DTNB and 0.017 mL of acetylthiocholine as above-described. Plots of enzyme activity for each compound expressed as percentage of the dialyzed free enzyme activity against time of dialysis were built for each inhibitor.

As the enzyme incubated with **18** was still inhibited after 48 h of dialysis, after dilution a linear plot was obtained for up to 5 h, according to the following expression

$$\ln(v_\infty - v_0) - \ln(v_\infty - v_t) = k_3 t$$

were v_∞ is the activity of the free reference enzyme submitted to dialysis and v_0 and v_t correspond to the residual carbamoylated enzyme activity at $t = 0$ and t. The decarbamoylation constant (k_3) was calculated by the slope of the plot.

Inhibition of AChE in Rat Cerebral Cortex. Assays for in vitro inhibition of AChE activity in rat cortex were conducted using a method modified from previously published ones.[25−29] Briefly, brain cortical tissue was dissected out from adult wistar rats and stored frozen for several weeks. Frozen tissues were then suspended in phosphate buffer (25 mM, pH 7.4) to a ratio of 1:200 wet weight/vol and homogenized. The homogenates were incubated at 37 °C for 5 min and then centrifuged at 50000*g* for 15 min at 4 °C. The pellets were then suspended in the initial volume of phosphate buffer and used for AChE assays. This partial fractionation allows elimination of endogenous substrate, which would interfere with the assay, and leads to an enrichment of AChE activity. For enzymatic assay, 100 μL of the AChE-enriched fraction was added to a tube containing 50 μL of test compound in PBS (pH 7.4) and 50 μL of tritiated ACh (specific activity 4.56 mCi/mmol, final ACh concentration 0.4 mM, in PBS, pH 7.4). Such conditions were found to be optimal to study competitive inhibition. Experiments conducted at the saturating concentration of substrate required a dilution of tritiated ACh with cold ACh to a specific activity of 124 μCi/mmol (final ACh concentration 2 mM). The enzymatic reaction was allowed to proceed for 15 min at 37 °C and stopped with 200 μL of blocking solution (94.5 g of chloroacetic acid and 116.88 g of sodium chloride in 1 L of a 0.5 M NaOH solution). After the addition of a mixture of isoamylic alcohol/toluene to the reaction tube, the amount of ^3H-acetate formed was measured in a liquid scintillation counter as the amount of radioactivity present in the organic phase. Blanks and positive controls were performed in the presence or absence of physostigmine (10 μL), respectively. Data were obtained from at least three determinations conducted in duplicate and the IC_{50} values determined with the use of a computed-assisted curve-fitting program (EBDA).[30]

^3H-acetylcholine was from Dupont NEN, all the other reagents were from Sigma Chemical Co.

Computational Methods. Molecular dynamics (MD) simulations were performed using the united-atom AMBER* force field implemented in the MacroModel Ver. 5.5 program,[31] running on a Silicon Graphics Indigo2 workstation. The coordinates of the protein were obtained from the X-ray structure of AChE isolated from *T. californica*[6] and retrieved from the Brookhaven Protein Data Bank (entry 1ace); Phe330 was replaced by Tyr with the same conformation.

Polar and aromatic hydrogens were added to the protein, while the aliphatic portions of the macromolecule were treated using the united-atom model of AMBER.[32] The inhibitor **8** was docked into the enzyme by building a tetrahedral complex between the Ser200 Oγ and the carbamate group; the protonated amine group was placed at van der Waals distance from Trp84, and the xanthenonyloxyalkyl substituent was positioned within the gorge in such a way as to avoid unfavorable contacts.

In setting up the criteria for building the molecular model, we defined a core of atoms around the active site and a shell surrounding the core, on which the minimizations and the dynamics simulations were carried out. The core was made up by any atom of the protein within 10 Å from any atom of the inhibitor; the shell contained any atom within 3 Å from any atom of the core. All the atoms within the core were unconstrained, while atoms in the shell were constrained by applying an energy penalty force constant of 100 kJ/Å^2 mol^{-1}. Atoms beyond the shell were maintained at the X-ray coordinates.

On this system, an initial minimization (1500 steps, steepest descent) and a subsequent temperature constant MD simulation (80 ps, 298 K, 1.5 fs time step) were carried out. An equilibration time of 30 ps was allowed before starting the data collection. The SHAKE algorithm[33] was used to constrain all bonds involving hydrogens at their equilibrium values. The last conformation sampled by MD was energy minimized first by steepest descent (1500 steps) and then by conjugate gradient with a derivative convergence criterion of 0.05 kJ/Å^2 mol^{-1}.

Acknowledgment. Investigation supported by University of Bologna (funds for selected research topics) and by MURST.

References

(1) Varghese, J.; Lieberburg, I.; Thorsett, E. D. Alzheimer's Disease: Current Therapeutic Approaches. *Ann. Rep. Med. Chem.* **1993**, *28*, 197−206.

(2) Summers, W. K.; Majovski, L. V.; Marsh, G. M.; Tachiki, K.; Kling, A. Oral Tetrahydroaminoacridine in Long-term Treatment of Senile Dementia, Alzheimer Type. *N. Engl. J. Med.* **1986**, *315*, 1241−1245.

(3) (a) Shutske, G. M.; Pierrat, F. A.; Cornfeldt, M. L.; Szewczak, M. R.; Huger, F. P.; Bores, G. M.; Haroutunian, V.; Davis, K. L. (±) 9-Amino-1,2,3,4-tetrahydroacridin-1-ol. A Potential Alzheimer's Disease Therapeutic of Low Toxicity. *J. Med. Chem.* **1988**, *31*, 1278−1279. (b) Nabeshima, T.; Yoshida, S.; Kameyama, T. Effects of the Novel Compound NIK-247 on Impairment of Passive Avoidance Response in Mice. *Eur. J. Pharmacol.* **1988**, *154*, 263−269. (c) Shutske, G. M.; Pierrat, F. A.; Kapples, K. J.; Cornfeldt, M. L., Szewczak, M. R.; Huger, G. M.; Haroutunian, V.; Davis, K. L. 9-Amino-1,2,3,4-tetrahydroacridin-1-ols: Synthesis and Evaluation as Potential Alzheimer's Disease Therapeutics. *J. Med. Chem.* **1989**, *32*, 1805−1813.

(4) (a) Brufani, M.; Castellano, C.; Marta, M.; Oliviero, A.; Pagella, P. G.; Pavone, F.; Pomponi, M.; Rugarli, P. L. A Long-Lasting Cholinesterase Inhibitor Affecting Neural and Behavioral Processes. *Pharmacol. Biochem. Behav.* **1987**, *26*, 625−629. (b)

Atack, J. R.; Yu, Q. S.; Soncrant, T. T.; Brossi, A.; Rapoport, S. I. Comparative Inhibitory Effects of Various Physostigmine Analogues Against Acetyl- and Butyrylcholinesterases. *J. Pharmacol. Exp. Ther.* **1989**, *249*, 194−202. (c) Greig, N. H.; Pei, X.-F.; Soncrant, T. T.; Ingram, D. K.; Brossi, A. Phenserine and Ring C Hetero-Analogues: Drug Candidates for the Treatment of Alzheimer's Disease. *Med. Res. Rev.* **1995**, *15*, 3−31.

(5) (a) Sugimoto, H.; Tsuchiya, Y.; Sugumi, H.; Higurashi, K.; Karibe, N.; Iimura, Y.; Sasaki, A.; Araki, S.; Yamanishi, Y.; Yamatsu, K. Novel Piperidine Derivatives. Synthesis and Anti-acetylcholinesterase Activity of 1-Benzyl-4-[2-(N-benzoylamino)-ethyl]-piperidine Derivatives. *J. Med. Chem.* **1990**, *33*, 1880−1887. (b) Sugimoto, H.; Sugumi, H.; Higurashi, K.; Karibe, N.; Iimura, Y.; Sasaki, A.; Araki, S.; Yamanishi, Y.; Yamatsu, K. Synthesis and Structure−Activity Relationships of Acetylcholinesterase Inhibitors: 1-Benzyl-4-(2-phthalimidoethyl)piperidine and Related Derivatives. *J. Med. Chem.* **1992**, *35*, 4542−4548. (c) Sugimoto, H.; Iimura, Y.; Yamanishi, Y.; Yamatsu, K. Synthesis and Anti-Acetylcholinesterase Activity of 1-Benzyl-[(5,6-dimethoxy-1-indanon-2-yl)methyl]piperidine Hydrochloride (E2020) and Related Compounds. *Bioorg. Med. Chem. Lett.* **1992**, *2*, 871−876.

(6) Sussman, J. L.; Harel, M.; Frolow, F.; Oefner, C.; Goldman, A.; Toker, L.; Silman, I. Atomic Structure of Acetylcholinesterase from *Torpedo Californica*: A Prototypic Acetylcholine-Binding Protein. *Science* **1991**, *253*, 872−879.

(7) Chen, Y. L.; Liston, D.; Nielsen, J.; Chapin, D.; Dunaiskis, A.; Hedberg, K.; Ives, J.; Johnson, J. Jr.; Jones, S. Synthesis and Anticholinesterase Activity of Tetrahydrobenzazepine Carbamates. *J. Med. Chem.* **1994**, *37*, 1996−2000.

(8) Ishihara, Y.; Kato, K.; Goto, G.; Central Cholinergic Agents. I. Potent Acetylcholinesterase Inhibitors, 2-[ω-[N-Alkyl-N-(ω-phenylalkyl)amino]alkyl]-1H-isoindole-1,3(2H)-diones, Based on a New Hypothesis of the Enzyme's Active Site. *Chem. Pharm. Bull.* **1991**, *39*, 3225−3235.

(9) Valenti, P.; Rampa, A.; Bisi, A.; Fabbri, G.; Andrisano, V.; Cavrini, V. Cholinergic Agents. Synthesis and Acetylcholinesterase Inhibitory Activity of Some ω-[*N*-Methyl-N-(3-alkylcarbamoyloxyphenyl)methyl]aminoalkoxyxanthen-9-ones. *Med. Chem. Res.* **1995**, *5*, 255−264.

(10) Pomponi, M.; Giardina, B.; Gatta, F.; Larta, M. Physostigmine and Tetrahydroaminoacridine Analogues as Alternative Drugs for the Treatment of Alzheimer's Disease. *Med. Chem. Res.* **1992**, *2*, 306−327.

(11) Da Re, P.; Sagramora, L.; Mancini, V.; Valenti, P.; Cima, L. Central Nervous System Stimulants of the Xanthone Group. *J. Med. Chem.* **1970**, *13*, 527−531.

(12) Da Re, P.; Valenti, P.; Borraccini, A.; Primofiore, G. P. β-Adrenergic Blocking Agents of the Chromone and Xanthone Groups. *J. Med. Chem.* **1972**, *15*, 198−199.

(13) Gaion, R. M.; Valenti, P.; Montanari, P.; Da Re, P. Xanthone Analogues of Clofibrate. Synthesis and Biological Evaluation as Antagonists of Lipolysis in Vitro. *Arzneim. Forsch./Drug Res.* **1982**, *32*, 499−502.

(14) Valenti, P.; Chiarini, A.; Gasperi, F.; Budriesi, R. Xanthone 1,4-Dihydropyridine Derivatives with a Potent Selective Bradycardic Effect. *Arzneim. Forsch./ Drug Res.* **1990**, *40*, 122−125.

(15) Valenti, P.; Recanatini, M.; Da Re, P.; Galimbeni, W.; Avanzi, N.; Filippeschi, S. Xanthone Analogues of Geiparvarin. *Arch. Pharm.* **1985**, *318*, 923−926.

(16) Valenti, P.; Da Re, P.; Rampa, A.; Montanari, P.; Carrara, M.; Cima, L. Benzo-γ-pyrone Analogues of Geiparvarin: Synthesis and Biological Evaluation Against B16 Melanoma Cells. *Anti-Cancer Drug Design*, **1993**, *8*, 349−360.

(17) Valenti, P.; Fabbri, G.; Rampa, A.; Bisi, A.; Gobbi, S.; Da Re, P.; Carrara, M.; Sgevano, A.; Cima, L. Synthesis and Antitumor Activity of Some Analogues of Flavone Acetic Acid. *Anti-Cancer Drug Des.* **1996**, *11*, 243−252.

(18) Recanatini, M.; Cavalli, A.; Hansch, C. A Comparative QSAR Study of Acetylcholinesterase Inhibitors Currently Studied for the Treatment of Alzheimer's Disease. *Chem. Biol. Interact.* **1997**, *105*, 199−228.

(19) Verloop, A.; Hoogenstraaten, W.; Tipker, J. *Drug Design*; Academic Press: New York, 1976; Vol. VII, pp 165−207.

(20) Soreq, H.; Ben-Aziz, R.; Prody, C. A.; Seidman, S.; Gnatt, A.; Neville, L.; Lieman-Hurwitz, J.; Lev-Lehman, E.; Ginzberg, D.; Lapidot-Lifson, Y.; Zakut, H. Molecular Cloning and Construction of the Coding Region for Acetylcholinesterase Reveals a G+C-Rich Attenuating Structure. *Proc. Natl. Acad. Sci. U.S.A.* **1990**, *87*, 9688−9692.

(21) Yamamoto, Y.; Ishihara, Y.; Kuntz, I. D. Docking Analysis of a Series of Benzylamino Acetylcholinesterase Inhibitors with a Phthalimide, Benzoyl, or Indanone Moiety. *J. Med. Chem.* **1994**, *37*, 3141−3153.

(22) Jorgensen, W. L.; Severance, D. L. Aromatic−Aromatic Interactions: Free Energy Profiles for the Benzene Dimer in Water, Chloroform, and Liquid Benzene. *J. Am. Chem. Soc.* **1990**, *112*, 4768−4774.

(23) (a) Nishioka, T.; Kitamura, K.; Fujita, T.; Nakajima, M. Kinetic Constants for the Inhibition of Acetylcholinesterase by Phenyl Carbamates. *Pestic. Biochem. Physiol.* **1976**, *6*, 320−337. (b) O'Brien, R. D. Kinetics of the Carbamylation of Cholinesterase. *Mol. Pharmacol.* **1968**, *4*, 121−130. (c) Wilson, I. B.; Hatch, M. A.; Ginsburg, S. Carbamylation of Acetylcholinesterase. *J. Biol. Chem.* **1960**, *235*, 2312−2315.

(24) Segel, I. H. *Biochemical Calculations*; Wiley & Sons: New York, 1976.

(25) Ellman, G. L.; Courtney, K. D.; Andres, V.; Featherstone, R. M. A New and Rapid Colorimetric Determination of Acetylcholinesterase Activity. *Biochem. Pharmacol.* **1961**, *7*, 88−95.

(26) Chen, Y. L.; Nielsen, J.; Hedberg, K.; Dunaiskis, A.; Jones, S.; Russo, L.; Johnson, J.; Ives, J.; Liston, D. Synthesis, Resolution, and Structure−Activity Relationships of Potent Acetylcholinesterase Inhibitors: 8-Carbaphysostigmine Analogues. *J. Med. Chem.* **1992**, *35*, 1429−1434.

(27) Potter, L. T. A Radiometric Microassay of Acetylcholinesterase. *J. Pharm. Exp. Ther.* **1967**, *156*, 500−506.

(28) Johnson, C. D.; Russel, R. L. A Rapid, Simple Radiometric Assay for Cholinesterase, Suitable for Multiple Determinations. *Anal. Biochem.* **1975**, *64*, 229−238.

(29) Thomsen, T.; Zendeh, B.; Fischer, J. P.; Kewitz, H. In Vitro Effects of Various Cholinesterase Inhibitors on Acetyl- and Butyrylcholinesterase of Healthy Volunteers. *Biochem. Pharmacol.* **1991**, *41*, 139−141.

(30) McPherson, G. I. Ligand, Release 2.01. Cambridge, Elsevier Biosoft, 1987.

(31) Mohamadi, F.; Richards, N. G. J.; Guida, W. C.; Liskamp, R. M. J.; Lipton, M. A.; Caulfield, C. E.; Chang, G.; Hendrickson, T. F.; Still, W. C. MacroModel − an Integrated Software System for Modeling Organic and Bioorganic Molecules Using Molecular Mechanics. *J. Comput. Chem.* **1990**, *11*, 440−467.

(32) Weiner, S. J.; Kollman, P. A.; Case, D. A.; Singh, U. C.; Ghio, C.; Alagona, G.; Profeta, S., Jr.; Weiner, P. A New Force Field for Molecular Mechanical Simulation of Nucleic Acids and Proteins. *J. Am. Chem. Soc.* **1984**, *106*, 765−784.

(33) Ryckaert, J. P. Special Geometrical Constraints in the Molecular Dynamics of Chain Molecules. *Mol. Phys.* **1985**, *55*, 549−556.

JM9810046